Pis'ma v ZhETF, vol. 97, iss. 8, pp. 566 – 573 April 25

ПО ИТОГАМ ПРОЕКТОВ
РОССИЙСКОГО ФОНДА ФУНДАМЕНТАЛЬНЫХ ИССЛЕДОВАНИЙ
Проект РФФИ # 10-02-00016а

Quantum field theory and the new phase of studies of hadron production mechanisms caused by high level of accuracy of experiments

N. N. Achasov[1)], *A. V. Kiselev, A. A. Kozhevnikov, G. N. Shestakov*

Laboratory of Theoretical Physics, Sobolev Institute of Mathematics, SB of the RAS, 630090 Novosibirsk, Russia

Submitted 28 March 2013

Modern experiment allows to solve many problems of hadron physics both rather old and new ones. In particular, during implementation of the project, mechanisms of production of the light scalar mesons in photon-photon collisions are installed, i.e., the question raised thirty years ago is solved.

DOI: 10.7868/S0370274X13080122

1. Introduction. An analysis of the high-statistics data on two-photon production of light scalar mesons, obtained by the Belle collaboration with B-factory in Japan [1–4], revealed that their production mechanisms are four-quark transitions caused by rescatterings, which is, in turn, an important argument in favor of four-quark nature of light scalar mesons [5–10]. In particular, we show that the prediction of the ideal two-quark model for the ratio of the widths of the two-photon decay equal to 25/9 for the light scalar $f_0(980)$ and $a_0(980)$ mesons is excluded by experiment [9], while for the two-quark tensor partners $f_2(1270)$ and $a_2(1320)$ is well satisfied.

It is shown that high-statistics research of light scalar mesons in photon-photon collisions: 1) in reactions $\gamma\gamma \to K\bar{K}$ near the threshold, 2) and also in reactions $\gamma^*(Q^2)\gamma \to \pi^0\pi^0$ and $\gamma^*(Q^2)\gamma \to \pi^0\eta$, will allow to receive the valuable information about the nature of light scalar mesons. In particular, it is shown that in case of their four-quark nature should be expected strong suppression of the Born contribution to the reaction $\gamma\gamma \to K^-K^+$ about the threshold [11], and in reactions $\gamma^*(Q^2)\gamma \to \pi^0\pi^0$ and $\gamma^*(Q^2)\gamma \to \pi^0\eta$ a swift falling of the cross sections with increase of the photon virtuality Q^2 [9].

A scenario is suggested, in which a resonance in the reaction $\gamma^*(Q^2)\gamma \to K\bar{K}\pi$ is caused not by the production of the axial-vector meson $f_1(1420)$, as is commonly believed, but by the production of the pseudoscalar meson $\eta(1475)$ [12–14]. Verification of this scenario, including in the decays of heavy quarkonium, will provide valuable information on the pseudoscalar glueballs.

It is constructed an analytical model of the amplitude $\pi\pi$ scattering involving light scalar mesons, which describe the experimental data and theoretical calculations based on chiral expansion, the dispersion relations and Roy equations [15–17]. The model fits well with the four-quark scenario for light scalar mesons.

The mechanism of production of light scalar mesons in semileptonic decays of the heavy quarkonium $D_s^+ = c\bar{s}$ is investigated [18]. It is shown that the lightest scalar meson $\sigma(600)$ contains almost no strange quark pairs, $s\bar{s}$, and their share of $f_0(980)$ meson does not exceed 30 percent. Thus semileptonic decays support existing arguments in favor of the dominant role of the four-quark component in the $\sigma(600)$ and $f_0(980)$ mesons. The program of study of light scalar mesons in semileptonic decays of D^+ and D^0 mesons (or D^- and $\bar{D}^0$) is proposed [18].

Interference phenomena observed in the $\psi(3770)$ resonance region in the $e^+e^- \to D\bar{D}$ reactions are studied in the models that satisfy the elastic unitarity condition [19]. A good description of the current data is obtained. Selection of theoretical models can be done by comparing their predictions with the data on the form of the $\psi(3770)$ peak in the channels $e^+e^- \to \gamma\chi_{c0}$, $J/\psi\eta$, $\phi\eta$, etc.

[1)]e-mail: achasov@math.nsc.ru

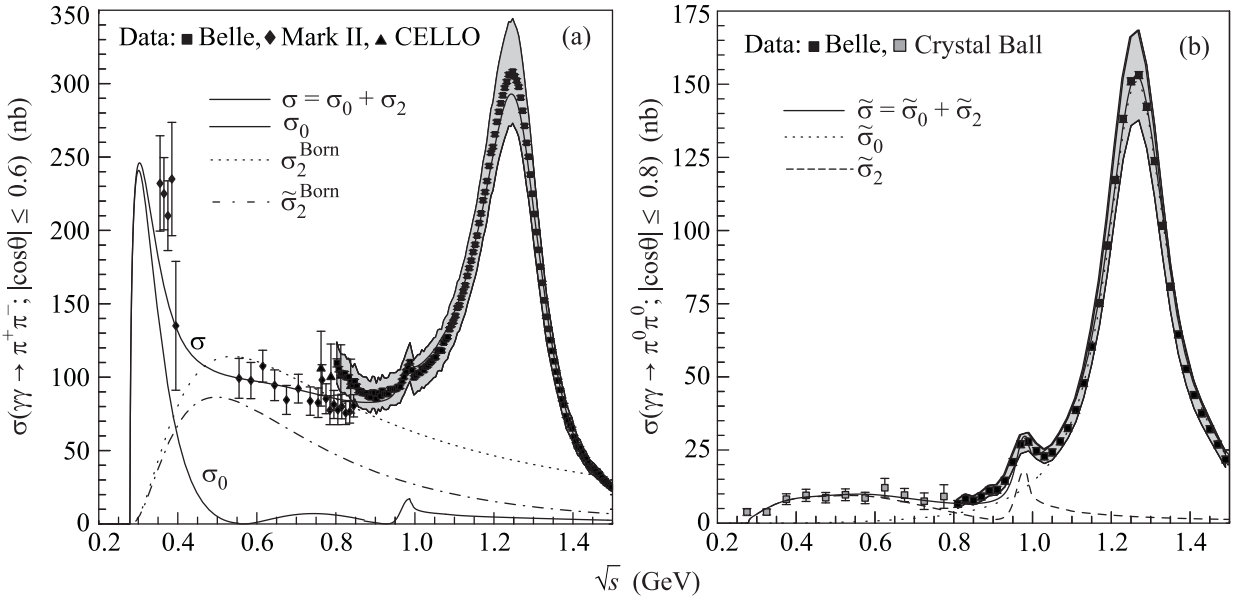

Fig. 1. Our combined description [9] of the data on the $\gamma\gamma \to \pi^+\pi^-$ (a) and $\gamma\gamma \to \pi^0\pi^0$ (b) reaction cross sections. σ, σ_0, σ_2, $\sigma_2^{\rm Born}$, $\widetilde{\sigma}_2^{\rm Born}$ denote cross sections for $\gamma\gamma \to \pi^+\pi^-$ and $\widetilde{\sigma}$, $\widetilde{\sigma}_0$, $\widetilde{\sigma}_2$ for $\gamma\gamma \to \pi^0\pi^0$ (for further details see Ref. [9]). The shaded bands correspond to the Belle data [2, 3] with their statistical and systematic errors (added up quadratically)

Generalized Hidden Local Symmetry (GHLS) model as the chiral model of pseudoscalar, vector, and axial vector mesons, is confronted the ALEPH data on the decay $\tau^- \to \pi^-\pi^-\pi^+\nu_\tau$. The modifications of GHLS based on inclusion of heavier axial vector mesons are studied [20, 21]. It is shown that the scheme with two additional axial vector isovector mesons with masses $m_{a_1'} = 1.59$ GeV and $m_{a_1''} = 1.88$ GeV gives a good description of the ALEPH data.

An analytical form factor of the pion, inspired by field theory, is constructed [22–24]. It describes very well the current high-statistics data, obtained in the time-like region by SND, CMD-2, KLOE, BABAR collaborations and in the space-like region by NA7 collaboration (CERN) for $-10\,{\rm GeV}^2 < s < 1\,{\rm GeV}^2$. The charge pion radius is calculated.

The new sum rules for the Z-boson radiative decays into heavy quarkonia are studied and shown that the decay intensities $BR(Z \to \gamma J/\psi(1S)) \sim BR(Z \to \to \gamma\Upsilon(1S)) \sim 10^{-6}$ are possible [25, 26] and probably can be measured at the Large Hadron Collider.

2. Light scalar mesons in $\gamma\gamma$ collisions. A major contribution to understanding of the nature of light scalar mesons $\sigma(600)$, $f_0(980)$, and $a_0(980)$, which are candidates for four-quark states, comes from the physics of photon-photon collisions, where high-statistics data have recently been obtained (see, e.g., review [9]). In the series of measurements of the cross sections for the $\gamma\gamma \to \pi^+\pi^-$ [1, 2], $\gamma\gamma \to \pi^0\pi^0$ [3], and $\gamma\gamma \to \pi^0\eta$ [4] reactions, performed at the KEKB e^+e^- collider, the Belle collaboration accumulated statistics two or three orders of magnitude higher than that in pre-B-factory experiments (see Figs. 1 and 2; $\sqrt{s}$ is the invariant mass of the final meson system). Really, after analyses of the Belle data, the physics of two-photon decays of light scalar mesons can be more clearly delineated [5–10]. The mechanism of their decays into $\gamma\gamma$ differs from the decay mechanism of the classical tensor $q\bar{q}$-meson, i.e., direct $q\bar{q} \to \gamma\gamma$ annihilation. The decays of light scalar mesons into $\gamma\gamma$, suppressed in comparison with those of tensor mesons, are mediated through the rescattering mechanisms, i.e., four-quark transitions $\sigma(600) \to \pi^+\pi^- \to \gamma\gamma$, $f_0(980) \to K^+K^- \to \gamma\gamma$, $a_0(980) \to (K^+K^-, \pi^0\eta) \to \gamma\gamma$, etc., whereas the direct coupling constants of $\sigma(600)$, $f_0(980)$, and $a_0(980)$ to photons are small. Such a picture is consistent with available data and confirms the $q^2\bar{q}^2$-nature of light scalar mesons. It is impossible to comprehensively characterize the coupling between scalar mesons and photons (by analogy with tensor mesons) by the values of the $\Gamma_{0^{++}\to\gamma\gamma}(m^2_{0^{++}})$ constants. As an adequate working characteristic of the coupling between $f_0(980)$ and $\gamma\gamma$, we determine the $f_0(980) \to \to \gamma\gamma$ decay width averaged over the resonance mass distribution in the $\pi\pi$ channel: $\langle\Gamma_{f_0\to\gamma\gamma}\rangle_{\pi\pi}$. For our combined fit (see Fig. 1), $\langle\Gamma_{f_0\to\gamma\gamma}\rangle_{\pi\pi} \approx 0.19$ keV. Taking into account that the $2m_\pi < \sqrt{s} < 0.8$ GeV region is dominated by the wide $\sigma(600)$ resonance, we obtain $\langle\Gamma_{\sigma\to\gamma\gamma}\rangle_{\pi\pi} \approx 0.45$ keV. Analogously, for the $a_0(980) \to$

$\gamma\gamma$ decay width averaged over the resonance mass distribution in the $\pi\eta$ channel (see Fig. 2), we estimate

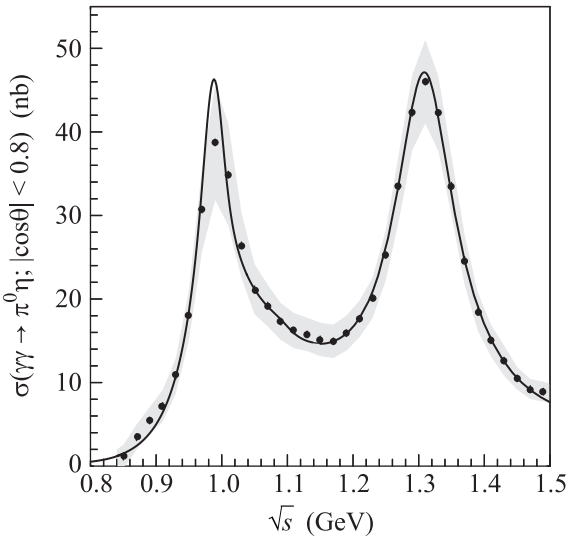

Fig. 2. Our fit [5] to the Belle data [4] on the $\gamma\gamma \to \pi^0\eta$ reaction cross section. The shaded band shows the size of the systematic error in data

$\langle\Gamma_{a_0(980)\to\gamma\gamma}\rangle_{\pi\eta} \approx 0.4$ keV. As concerns the prediction of the ideal $q\bar{q}$ model for the two-photon decay widths of $f_0(980)$ and $a_0(980)$ mesons, $\Gamma_{f_0\to\gamma\gamma}/\Gamma_{a_0\to\gamma\gamma} = 25/9$, it is excluded by experiment.

High-statistical data on the $\gamma\gamma \to K^-K^+$ and $\gamma\gamma \to$ $\to K^0\bar{K}^0$ reactions constitute the last missing link in investigations of light scalar mesons $f_0(980)$ and $a_0(980)$ in photon-photon collisions. It is expected that the manifestation of the four-quark structure of the $f_0(980)$ and $a_0(980)$ resonances in these reactions will be very peculiar [9, 11]. According to experiments, the cross sections for $\gamma\gamma \to K^+K^-$ and $\gamma\gamma \to K^0_SK^0_S$ reactions in the range of 1.2 GeV $< \sqrt{s} <$ 1.7 GeV are saturated by the contributions from classical tensor resonances $f_2(1270)$, $a_2(1320)$, and $f_2'(1525)$ produced in states with a helicity of $\lambda = \pm 2$. The Born contribution largely overestimates the background under the tensor meson peaks in K^+K^- (see Fig. 3). However, the S-wave resonant interaction between the K^+ and K^- mesons in the final state compensates a significant part of this background in a wide $\sqrt{s}$ range. This is the result of the strong coupling of the $f_0(980)$ and $a_0(980)$ resonances with the $K\bar{K}$ channels, which is natural in the four-quark scheme. Thus, scalar contributions of 5–10 nb can be detected in the cross section for the $\gamma\gamma \to K^+K^-$ reaction in the range of $2m_{K^+} < \sqrt{s} < 1.1$ GeV (see Fig. 3). The $\gamma\gamma \to K^0\bar{K}^0$ cross section is expected to be $\lesssim 1$ nb. The possibility of explaining the suppression of the large S-wave Born contribution to $\gamma\gamma \to K^+K^-$ by the

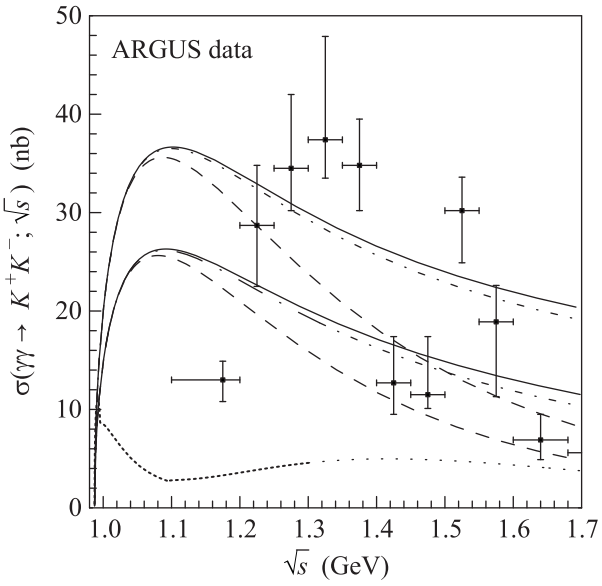

Fig. 3. The upper (lower) dashed, dashed-dot, and solid curves correspond to the Born $\gamma\gamma \to K^+K^-$ cross section for the elementary (modified by the form factor) one-kaon exchange with $\lambda J = 00$, $|\lambda|J = 00 + 22$, and to the total cross section, respectively. Here λ is the total helicity of initial photons and J is their total angular momentum. The dotted curve is our estimate of the S-wave cross section for the $\gamma\gamma \to K^+K^-$ reaction

contribution from the $f_0(980)$ and $a_0(980)$ resonances, $\gamma\gamma \to K^+K^- \to [f_0(980) + a_0(980)] \to K^+K^-$, would indicate in favor of the dominant role of four-quark transitions (i.e. rescattering mechanisms) in the $f_0(980) \to \gamma\gamma$ and $a_0(980) \to \gamma\gamma$ decays and, correspondingly, in favor of the $q^2\bar{q}^2$ nature of the $f_0(980)$ and $a_0(980)$ states.

3. $\eta(1475)$ versus $f_1(1420)$. The reactions $\gamma\gamma^*(Q^2) \to K^0_SK^\pm\pi^\mp$ have been investigated parallel with the reactions $\gamma\gamma \to K^0_SK^\pm\pi^\mp$. A clear resonance signal in the $\gamma\gamma^*(Q^2) \to K^0_SK^\pm\pi^\mp$ cross sections has been found in the $K^0_SK^\pm\pi^\mp$ invariant mass range $1.35\,\text{GeV} < \sqrt{s} < 1.55\,\text{GeV}$ for $Q^2 \neq 0$ (in the photon virtuality region $0.04\,\text{GeV}^2 < Q^2 < (1\text{–}8)\,\text{GeV}^2$). The absence of the resonance signal in $\sigma(\gamma\gamma \to K^0_SK^\pm\pi^\mp)$ and its appearance in $\sigma(\gamma\gamma^*(Q^2) \to K^0_SK^\pm\pi^\mp)$ has led naturally to the hypothesis of the $J^P = 1^+$ $f_1(1420)$ resonance production, which is forbidden in two real photon collisions (for small Q^2, the $\gamma\gamma^*(Q^2) \to f_1(1420)$ transition amplitude is proportional to $\sqrt{Q^2}$). So far poor statistics in the existing experiments did not allow a determination of the spin-parity of this resonance structure directly with the angular distributions. In the works [12–14], we showed that, with the help of the $J^P = 0^-$ $\eta(1475)$ resonance and the generalized vector meson dominance model, we can explain simultaneously

the peak in the $\gamma\rho^0$ mass spectrum in the $J/\psi \to \gamma\gamma\rho^0$ decay, the pseudoscalar structures near thresholds in the $\rho\rho$ and $\omega\omega$ mass spectra in $J/\psi \to \gamma(\rho\rho, \omega\omega)$ decays, and the suppression of the $\eta(1475)$ signal in the reaction $\gamma\gamma \to K\bar{K}\pi$ and its appearance in $\gamma\gamma^*(Q^2) \to K\bar{K}\pi$ for $Q^2 \neq 0$. Our explanation might be rejected unambiguously by measuring the spin-parity of the signal in the region of 1475 MeV in the reaction $\gamma\gamma^*(Q^2) \to K\bar{K}\pi$, together with the disavowal of the pseudoscalar structures in the $\rho\rho$ and $\gamma\rho^0$ mass spectra in the $J/\psi \to \gamma\rho\rho$ and $J/\psi \to \gamma\gamma\rho^0$ decays.

4. Light scalar mesons in $\pi\pi$ scattering. We constructed the $\pi\pi$ scattering amplitude T_0^0 with regular analytical properties in the s complex plane, describing both experimental data and the results based on chiral expansion and Roy equations. Now the results obtained during development of our work are presented in the papers [15–17]. We dwell on questions dealing with the low $\sigma - f_0$ mixing, inelasticity description and the kaon loop model for the $\phi \to \gamma(\sigma + f_0)$ reaction, and show a number of new fits. In particular, we show that the minimization of the $\sigma - f_0$ mixing results in the four-quark scenario for light scalars: the $\sigma(600)$ coupling with the $K\bar{K}$ channel is suppressed relatively to the coupling with the $\pi\pi$ channel, and the $f_0(980)$ coupling with the $\pi\pi$ channel is suppressed relatively to the coupling with the $K\bar{K}$ channel.

Our model the S matrix of the $\pi\pi$ scattering is the product of the "resonance" and "elastic background" parts: $S_0^0 = S_0^{0\,\mathrm{back}}\, S_0^{0\,\mathrm{res}}$, and we introduced the special $S_0^{0\,\mathrm{back}}$ parametrization to obtain the correct T_0^0 analytical properties. The performed analysis shows that the scenario, based on the four-quark model, completely agrees with the current experimental data and theoretical requirements. We present for different fits of the data the $\sigma(600)$ and $f_0(980)$ poles, the residues of T_0^0, $\mathrm{Res}\, T_0^0$, and of the resonance part $T_0^{0\mathrm{Res}}$, $\mathrm{Res}\, T_0^{0\mathrm{Res}}$, in these poles on different sheets of the complex s plane depending on sheets of polarization operators for the $\pi\pi$, $K\bar{K}$, $\eta\eta$, $\eta\eta'$, and $\eta'\eta'$ channels. We also discuss the approximate character of the Roy equations, that take into account only the $\pi\pi$ decay channel, and note that efforts aiming the precise determination of the σ pole are not productive. The best way for understanding the nature of the light scalars is the investigation of their production mechanisms in physical processes. In this investigation we paid more attention to the inelasticity η_0^0 of $\pi\pi$ scattering, namely, we tried to reproduce the peculiar behavior near the threshold, indicated by the experimental data. Unfortunately, the current data have large errors, so the precise measurement of the inelasticity η_0^0 near 1 GeV in $\pi\pi \to \pi\pi$ would be very important.

5. Light scalars in semileptonic decays of charmed mesons. We study in Ref. [18] the mechanism of production of the light scalar mesons in the $D_s^+ \to \pi^+\pi^-\, e^+\nu$ decays: $D_s^+ \to s\bar{s}\, e^+\nu \to [\sigma(600) + f_0(980)]\, e^+\nu \to \pi^+\pi^-\, e^+\nu$, and we compare it with the mechanism of production of the light pseudoscalar mesons in the $D_s^+ \to (\eta/\eta')\, e^+\nu$ decays: $D_s^+ \to s\bar{s}\, e^+\nu \to (\eta/\eta')\, e^+\nu$. As Fig. 4 suggests, the

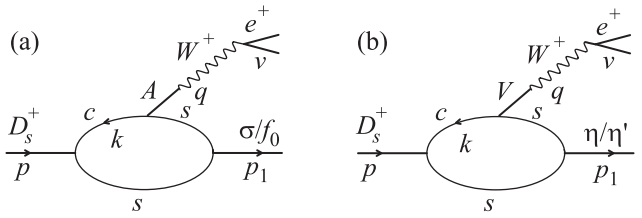

Fig. 4. The model of the $D_s^+ \to \sigma/f_0\, e^+\nu$ (a) and $D_s^+ \to (\eta/\eta')\, e^+\nu$ (b) decays

$D_s^+ \to s\bar{s}\, e^+\nu \to [\sigma(600) + f_0(980)]\, e^+\nu \to \pi^+\pi^-\, e^+\nu$ decay is the perfect probe of the $s\bar{s}$ component in the $\sigma(600)$ and $f_0(980)$ states. Our analysis shows that the $s\bar{s} \to \sigma(600)$ transition is negligibly small in comparison with the $s\bar{s} \to f_0(980)$ one. As far as we know, this is truly a new result, which agrees well with the decoupling of $\sigma(600)$ with the $K\bar{K}$ states, obtained in Ref. [17]. As for the $f_0(980)$ meson, the intensity of the $s\bar{s} \to f_0(980)$ transition makes near thirty percent from the intensity of the $s\bar{s} \to \eta_s$ ($\eta_s = s\bar{s}$) transition. So, the $D_s^+ \to \pi^+\pi^- e^+\nu$ decay supports the previous conclusions about a dominant role of the four-quark components $ud\bar{u}\bar{d}$ in the $\sigma(600)$ and $su\bar{s}\bar{u} + sd\bar{s}\bar{d}$ in $f_0(980)$. Our description of the $\pi^+\pi^-$ mass spectrum in the $D_s^+ \to \pi^+\pi^- e^+\nu$ decay is shown in Fig. 5. Certainly, there is an extreme need in experiment on the $D_s^+ \to \pi^+\pi^-\, e^+\nu$ decay with high statistics.

Of great interest is the experimental search for the decays $D^0 \to d\bar{u}\, e^+\nu \to a_0^-(980)\, e^+\nu \to \pi^-\eta\, e^+\nu$ and $D^+ \to d\bar{d}\, e^+\nu \to a_0^0(980)\, e^+\nu \to \pi^0\eta\, e^+\nu$ (or the charge conjugate ones), which will give the information about the $a_q^- = d\bar{u}$ (or $a_q^+ = u\bar{d}$) and $a_q^0 = (u\bar{u} - d\bar{d})/\sqrt{2}$ components in the $a_0^-(980)$ and $a_0^0(980)$ wave functions, respectively. No less interesting is also search for the decays $D^+ \to d\bar{d}\, e^+\nu \to [\sigma(600) + f_0(980)]\, e^+\nu \to \pi^+\pi^-\, e^+\nu$ (or the charge conjugate ones), which will give the information about the $\sigma_q = (u\bar{u} + d\bar{d})/\sqrt{2}$ and $f_{0q} = (u\bar{u} + d\bar{d})/\sqrt{2}$ components in the $\sigma(600)$ and $f_0(980)$ wave functions respectively.

6. Line shape of $\psi(3770)$ in $e^+e^- \to D\bar{D}$. In constructing the model describing the process

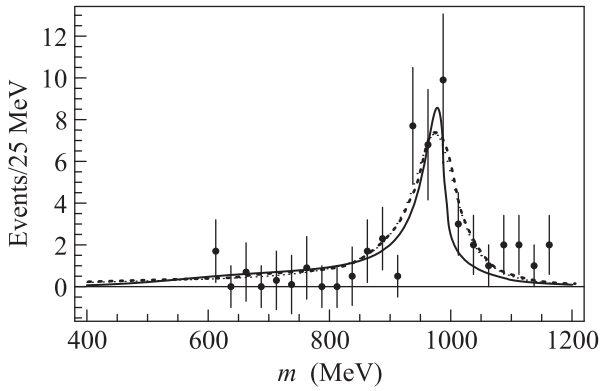

Fig. 5. The CLEO data on the invariant $\pi^+\pi^-$ mass (m) distribution for the $D_s^+ \to \pi^+\pi^- e^+\nu$ decay with the subtracted backgrounds. The dotted line is the fit from CLEO. Our theoretical curve is the solid line

$e^+e^- \to D\bar{D}$, one must keep in mind that we investigate above all the D-meson isoscalar electromagnetic form factor F_D^0. The phase of F_D^0 in the elastic region (i.e., between the $D\bar{D}$ (≈ 3.739 GeV) and $D\bar{D}^*$ (≈ 3.872 GeV) thresholds) is fixed by the unitarity condition equal to the phase δ_1^0 of the strong P-wave $D\bar{D}$ scattering amplitude T_1^0 in the channel with isospin $I=0$, i.e., $F_D^0 = e^{i\delta_1^0}\mathcal{F}_D^0$, where $\mathcal{F}_D^0$ and δ_1^0 are the real functions of energy. A similar representation of the amplitude $e^+e^- \to D\bar{D}$ used for the data description guarantees the unitarity requirement on the model level [19]. The sum of the $e^+e^- \to D\bar{D}$ reaction cross sections is given by $\sigma(e^+e^- \to D\bar{D}) = 8\pi\alpha^2 \left|F_D^0(s)\right|^2 \nu(s)/(3s^2)$, where s is the $D\bar{D}$-pair invariant mass square, $\nu(s) = [p_0^3(s) + p_+^3(s)]/\sqrt{s}$, $p_{0,+}(s) = \sqrt{s/4 - m_{D^{0,+}}^2}$ and $\alpha = e^2/4\pi = 1/137$. Below, for short $\psi(3770)$ is denoted as ψ''. Here we consider a simplest working variant of the model of the mixed ψ'' and $\psi(2S)$ resonances for the description of the interference pattern in the ψ'' region. Owing to the common $D^0\bar{D}^0$ and D^+D^- coupled channels, the ψ'' and the $\psi(2S)$ can transform into each other (i.e., mix); for example, $\psi'' \to D\bar{D} \to \psi(2S)$. The form factor F_D^0, corresponding to the contribution of the mixed ψ'' and $\psi(2S)$ resonances, is given by

$$F_D^0(s) = \frac{\mathcal{R}_{D\bar{D}}(s)}{D_{\psi''}(s)D_{\psi(2S)}(s) - \Pi_{\psi''\psi(2S)}^2(s)},$$

where $D_{\psi''}(s) = m_{\psi''}^2 - s - i\sqrt{s}\Gamma_{\psi''D\bar{D}}(s)$ and $D_{\psi(2S)}(s) = m_{\psi(2S)}^2 - s - i\sqrt{s}\Gamma_{\psi(2S)D\bar{D}}(s)$ are the inverse propagators of ψ'' and $\psi(2S)$, and $\Gamma_{\psi''D\bar{D}}(s) = g_{\psi''D\bar{D}}^2\,\nu(s)/(6\pi\sqrt{s})$ and $\Gamma_{\psi(2S)D\bar{D}}(s) = g_{\psi(2S)D\bar{D}}^2\,\nu(s)/(6\pi\sqrt{s})$ their decay widths, respectively. The amplitude $\Pi_{\psi''\psi(2S)}(s)$ describes the $\psi'' - \psi(2S)$ mixing. For simplicity we put $\mathrm{Re}\Pi_{\psi''\psi(2S)}(s) = 0$, i.e., we restrict ourselves only to the contribution of $\mathrm{Im}\Pi_{\psi''\psi(2S)}(s) = g_{\psi''D\bar{D}}g_{\psi(2S)D\bar{D}}\,\nu(s)/(6\pi)$ caused by the $\psi'' \to D\bar{D} \to \psi(2S)$ transitions via the real $D\bar{D}$ intermediate states. Then $\mathcal{R}_{D\bar{D}}(s)$ in the above equation for $F_D^0(s)$ takes the form: $\mathcal{R}_{D\bar{D}}(s) = (m_{\psi''}^2 - s)g_{\psi(2S)\gamma}g_{\psi(2S)D\bar{D}} + (m_{\psi(2S)}^2 - s)g_{\psi''\gamma}g_{\psi''D\bar{D}}$. Here the constants $g_{\psi''D\bar{D}}$, $g_{\psi(2S)D\bar{D}}$, and $g_{\psi''\gamma}$, $g_{\psi(2S)\gamma}$ characterize couplings of the ψ'', $\psi(2S)$ to the $D\bar{D}$ and virtual γ quantum, respectively. An example of the fit to the current data is shown in Fig. 6. It

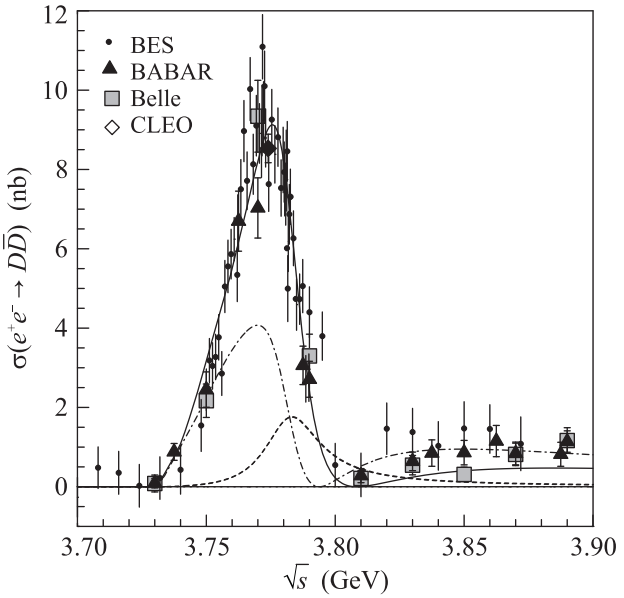

Fig. 6. The simplest variant of the model of the mixed ψ'' and $\psi(2S)$ resonances. The solid curve is the fit to the BES, CLEO, BABAR, and Belle data for $\sigma(e^+e^- \to D\bar{D})$. The dashed and dot-dashed curves show the contributions to the cross section from the ψ'' and $\psi(2S)$ production amplitudes proportional to the products of the coupling constants $g_{\psi''\gamma}g_{\psi''D\bar{D}}$ and $g_{\psi(2S)\gamma}g_{\psi(2S)D\bar{D}}$, respectively (see the text)

allows us to extract from experiment the coupling constant $g_{\psi(2S)D\bar{D}}^2/(4\pi) \approx 32$ which is inaccessible to direct measurements; we also obtain $g_{\psi''D\bar{D}}^2/(4\pi) \approx 16$. Owing to own clarity and simplicity the above variant of the $\psi'' - \psi(2S)$ mixing model can be tested, in the first place, in the treatment of new high-statistics data which can be expected from CLEO-c and BESIII on the $\psi(3770)$ shape in $e^+e^- \to D\bar{D}$. In Ref. [19], we also discuss the possibility of testing theoretical models by comparing their predictions with the relevant data on the shape of the $\psi(3770)$ peak in the non-$D\bar{D}$ mass spectra in $e^+e^- \to \gamma\chi_{c0}$, $J/\psi\eta$, $\phi\eta$, etc. The mass

spectra in the ψ'' region in the non-$D\bar{D}$ channels can be very diverse. Therefore, we should expect that the forthcoming data on such spectra, together with the $e^+e^- \to D\bar{D}$ data, will impose severe restrictions on the constructed dynamical models for the ψ'' resonance interfering with the background.

7. Improved the GHLS model. Generalized Hidden Local Symmetry (GHLS) model as chiral model of pseudoscalar, vector, and axial vector mesons and their interactions, based on nonlinear realization of chiral symmetry, has the virtue that the sector of electroweak interactions is introduced in such a way that the low energy relations in the sector of strong interactions are not violated upon inclusion of photons and electroweak gauge bosons. Earlier, the decays $\rho^0 \to \pi^+\pi^-$ and $\omega \to \pi^+\pi^-\pi^0$ were analyzed in the framework of GHLS. In Refs. [20, 21], we showed that the GHLS model is confronted the ALEPH data on the decay $\tau^- \to \pi^-\pi^-\pi^+\nu_\tau$. This decay incorporates the transition $W^- \to \pi^-\pi^-\pi^+$ given by the diagrams in Fig. 7. The simplest variant of GHLS with $m_{a_1} = 1.23$ GeV results in the spectrum shown with the dot-dashed line in Fig. 8. Upon variation of free parameters of the model with the single a_1 resonance contribution results in the curve drawn with the dashed line. It corresponds to $m_{a_1} \approx 1.54$ GeV and $\chi^2 = 690/(112\,\text{d.o.f})$. To improve the fit, heavier resonances a_1', a_1'' were included in a way analogous to $a_1(1260)$. Such a modification of the GHLS model yields a good description of the ALEPH data with $m_{a_1} = 1.332 \pm 0.015$ GeV, $m_{a_1'} = 1.59 \pm 0.01$ GeV, and $m_{a_1''} = 1.88 \pm 0.02$ GeV. Our best fit is shown in Fig. 8 by the solid curve. It corresponds to $\chi^2 = 79/(102\,\text{d.o.f})$.

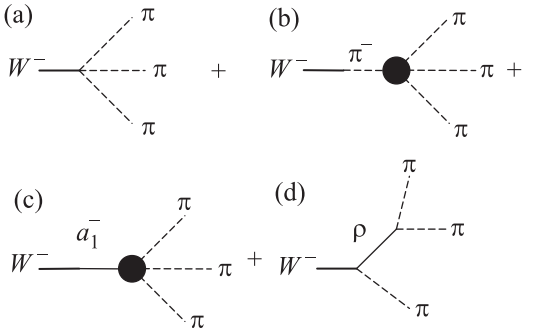

Fig. 7. Diagrams describing the transition $W^- \to \pi^-\pi^-\pi^+$

8. The π-meson analytical form factor. Based on the field-theory-inspired approach, a new expression for the pion form factor F_π is proposed [22–24]. It takes into account the pseudoscalar meson loops $\pi^+\pi^-$ and $K\bar{K}$ and the mixing of the $\rho(770)$ with the heavier $\rho(1450)$ and $\rho(1700)$ resonances. The expression possesses correct analytical properties and describes the data in the wide range of the energy squared $-10\,\text{GeV}^2 \le s \le 1\,\text{GeV}^2$. The quantity to fit is the $e^+e^- \to \pi^+\pi^-$ bare cross section

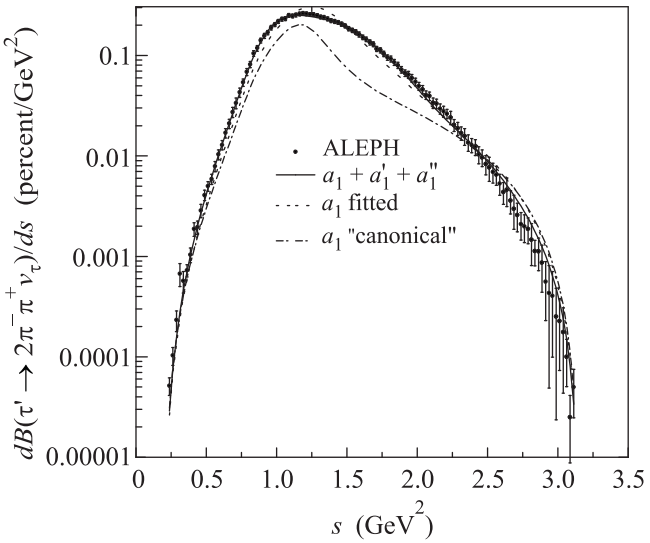

Fig. 8. Spectrum of $\pi^-\pi^-\pi^+$ in τ decay normalized to the branching fraction $B_{\tau^- \to \pi^-\pi^-\pi^+\nu_\tau}$

$$\sigma_{\text{bare}} = \frac{8\pi\alpha^2}{3s^{5/2}}|F_\pi(s)|^2 q_\pi^3(s)\left[1 + \frac{\alpha}{\pi}a(s)\right],$$

where $q_\pi(s) = \sqrt{s/4 - m_\pi^2}$ and the function $a(s)$ allows for the radiation of a photon by the final pions. The new expression for the pion form factor is given by

$$F_\pi(s) = (g_{\gamma\rho_1}, g_{\gamma\rho_2}, g_{\gamma\rho_3})G^{-1}\begin{pmatrix} g_{\rho_1\pi\pi} \\ g_{\rho_2\pi\pi} \\ g_{\rho_3\pi\pi} \end{pmatrix} + \\ + \frac{g_{\gamma\omega}\Pi_{\rho_1\omega}}{D_\omega\Delta}\left(g_{11}g_{\rho_1\pi\pi} + g_{12}g_{\rho_2\pi\pi} + g_{13}g_{\rho_3\pi\pi}\right).$$

It takes into account both the strong isovector $\rho(770) - -\rho(1450) - \rho(1700)$ mixing and the small $\rho(770) - \omega(782)$ one, automatically respects the current conservation condition $F_\pi(0) = 1$, and possesses correct analytical properties over entire s plane. The notations are as follows. $\rho_1 \equiv \rho(770)$, $\rho_2 \equiv \rho(1450)$, $\rho_3 \equiv \rho(1700)$;

$$G = \begin{pmatrix} D_{\rho_1} & -\Pi_{\rho_1\rho_2} & -\Pi_{\rho_1\rho_3} \\ -\Pi_{\rho_1\rho_2} & D_{\rho_2} & -\Pi_{\rho_2\rho_3} \\ -\Pi_{\rho_1\rho_3} & -\Pi_{\rho_2\rho_3} & D_{\rho_3} \end{pmatrix}$$

is the matrix of inverse propagators, g_{ij} are its matrix elements multiplied by $\Delta = \det G$; $g_{\gamma V} = m_V^2/g_V$ where g_V enters the leptonic partial widths like $\Gamma_{V\to e^+e^-} = 4\pi\alpha^2 m_V/3g_V^2$; $D_{\rho_i} = m_{\rho_i}^2 - s - \Pi_{\rho_i\rho_i}$ and $D_\omega = m_\omega^2 - s - i\sqrt{s}\Gamma_\omega(s)$. The diagonal polarization operators are

$\Pi_{\rho_i\rho_i} = g^2_{\rho_i\pi\pi}\left[\Pi(s, m^2_{\rho_i}, m^2_\pi) + \frac{1}{2}\Pi(s, m^2_{\rho_i}, m^2_K)\right]$, the non-diagonal ones are expressed through the diagonal one: $\Pi_{\rho_1\rho_{2,3}} = (g_{\rho_{2,3}\pi\pi}/g_{\rho_1\pi\pi})\Pi_{\rho_1\rho_1}$, $\Pi_{\rho_2\rho_3} = (g_{\rho_2\pi\pi}g_{\rho_3\pi\pi}/g^2_{\rho_1\pi\pi})\Pi_{\rho_1\rho_1} + sa_{23}$. The quantity a_{23} is one of free parameters. The explicit expressions for the polarization operators $\Pi_{\rho_i\rho_i}$ and $\Pi_{\rho_1\omega}$ and the detailed comparison of the model with the $e^+e^- \to \pi^+\pi^-$ data are presented in Refs. [22–24]. Our final results are shown in Fig. 9.

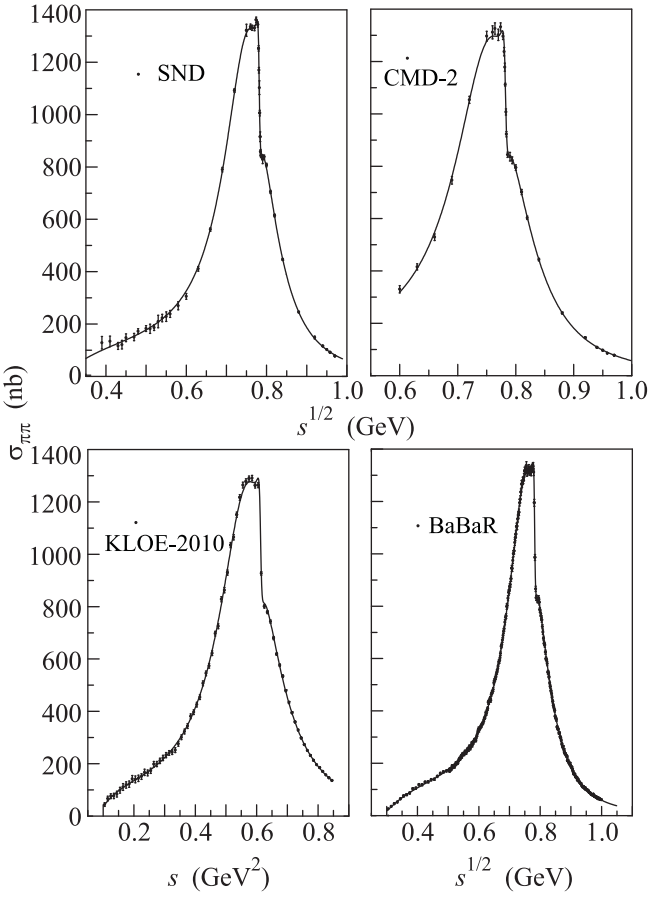

Fig. 9. The curves show the $e^+e^- \to \pi^+\pi^-$ bare cross section, calculated with the resonance parameters obtained from fitting of the SND, CMD-2, KLOE, and BABAR data, respectively

An important check of the expression for the pion form factor and the consistency of the fits is the continuation to the space-like region $s < 0$ accessible in the scattering processes. The results are shown in Fig. 10, where the comparison with the data is presented in the case of the resonance parameters found from fitting the BABAR data (see Fig. 9). As for the curves corresponding to the parameters found from fitting SND, CMD-2, and KLOE data, they coincide, within the errors, with the curve shown and hence are not drawn. We emphasize that the data for $s < 0$ are not included to the fits. Hence, a good agreement, demonstrated in Fig. 10 makes the evidence in favor of the validity of our model for the pion form factor.

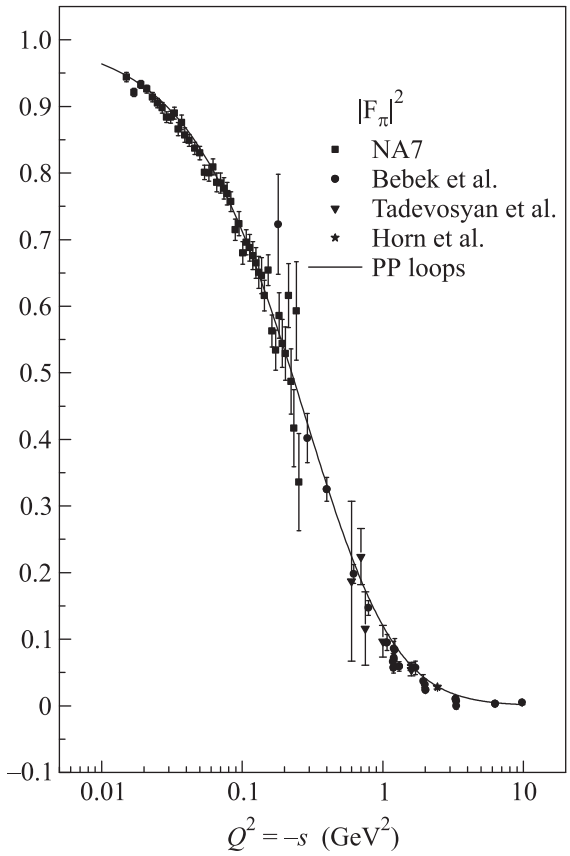

Fig. 10. The curve is our description of the pion form factor squared in the space-like region $s < 0$. For more details see Ref. [24]

9. New sum rules for the Z-boson radiative decays. The works [25, 26] are devoted to the $Z \to \to \gamma J/\psi$ and $Z \to \gamma\Upsilon$ decays. The main idea consists in the use of the invariant amplitudes of the triangle loop diagrams (see Fig. 11), describing the transition of the axial-vector current $\to q\bar{q} \to \gamma(k_1)\gamma(k_2)$ at $k_1^2 = 0$ and $k_2^2 \neq 0$, to construct the sum rules for the $Z \to c\bar{c}\,(\text{or}\,b\bar{b}) \to \gamma\gamma^*$ amplitude and its deriva-

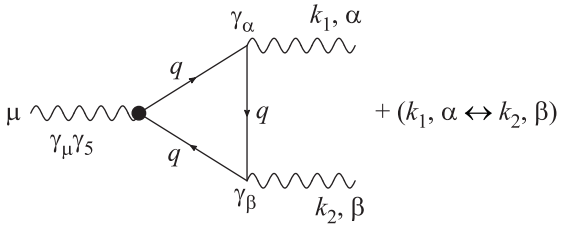

Fig. 11. The triangle diagrams

tive. Then the minima of the branching ratio sums ($\min \sum_V BR(Z \to \gamma V)$, where $V = \psi$ or Υ) are evaluated for different guesses as to saturation of the sum rules. Three assumption are investigated: i) the resonance saturation of the sum rule for the amplitude, ii) the resonance saturation of the sum rule for the amplitude derivative, and iii) the simultaneous resonance saturation of the amplitude and its derivative. It is shown that the resonance saturation of the sum rule for the amplitude derivative results in a reasonably small resonance contribution to the amplitude, whereas the resonance saturation of the sum rule for the amplitude results in an unacceptably large resonance contribution to the amplitude derivative. It is also shown that the simultaneous resonance saturation of the amplitude and its derivative allows to conclude that the resonance saturation of the sum rule for the amplitude derivative results in the minimum of $\min \sum_V BR(Z \to \gamma V)$, which agrees reasonably with the quark model prediction. Various deviations from this lower bound are considered. Specifically, it is discussed that the decay intensities $BR[Z \to \gamma J/\psi(1S)] \sim BR[Z \to \gamma\Upsilon(1S)] \sim 10^{-6}$ are possible [25, 26] and probably can be measured at the Large Hadron Collider.

10. Conclusion. We constructed a few models which are able to describe the modern high-statistics data. The obtained results are of practical importance. For example, the results on the pion electromagnetic form factor and the $\gamma\gamma \to K\bar{K}$ reactions near threshold are important for the physical programm of the VEPP-2000 accelerator which came into operation at Budker Institute of Nuclear Physics in Novosibirsk. The works on semileptonic decays of charmed mesons and the interference pattern in the $\psi(3770)$ region suggest the interesting programm of investigations at C/τ-factories.

Detailed references on the topics presented above may be found in the works [5–26].

This work was supported in part by RFBR, Grant # 13-02-00039, and Interdisciplinary project # 102 of Siberian division of RAS.

1. T. Mori, S. Uehara, Y. Watanabe et al., Phys. Rev. D **75**, 051101(R) (2007).
2. T. Mori, S. Uehara, Y. Watanabe et al., J. Phys. Soc. Jpn. **76**, 074102 (2007).
3. S. Uehara, Y. Watanabe, I. Adachi et al., Phys. Rev. D **78**, 052004 (2008).
4. S. Uehara, Y. Watanabe, H. Nakazawa et al., Phys. Rev. D **80**, 032001 (2009).
5. N. N. Achasov and G. N. Shestakov, Phys. Rev. D **81**, 094029 (2010).
6. N. N. Achasov and G. N. Shestakov, Pis'ma v ZhETF **92**, 3 (2010) [JETP Lett. **92**, 1 (2010)].
7. N. N. Achasov and G. N. Shestakov, Chinese Physics C **34**, 807 (2010).
8. N. N. Achasov, Physics of Particles and Nuclei **41**, 891 (2010).
9. N. N. Achasov and G. N. Shestakov, Usp. Fiz. Nauk **181**, 827 (2011) [Physics-Uspekhi **54**, 799 (2011)].
10. N. N. Achasov and G. N. Shestakov, Nucl. Phys. B (Proc. Suppl.) **225–227**, 135 (2012).
11. N. N. Achasov and G. N. Shestakov, Pis'ma v ZhETF **96**, 543 (2012) [JETP Lett. **96**, 493 (2012)].
12. N. N. Achasov and G. N. Shestakov, Pis'ma v ZhETF **94**, 13 (2011) [JETP Lett. **94**, 11 (2011)].
13. N. N. Achasov and G. N. Shestakov, Phys. Rev. D **84**, 034036 (2011).
14. N. N. Achasov and G. N. Shestakov, Nucl. Phys. B (Proc. Suppl.) **225–227**, 62 (2012).
15. N. N. Achasov and A. V. Kiselev, Phys. Rev. D **83**, 054008 (2011).
16. N. N. Achasov and A. V. Kiselev, Nucl. Phys. B (Proc. Suppl.) **225–227**, 14 (2012).
17. N. N. Achasov and A. V. Kiselev, Phys. Rev. D **85**, 094016 (2012).
18. N. N. Achasov and A. V. Kiselev, Phys. Rev. D **86**, 114010 (2012).
19. N. N. Achasov and G. N. Shestakov, Phys. Rev. D **86**, 114013 (2012).
20. N. N. Achasov and A. A. Kozhevnikov, Phys. Rev. D **82**, 076005 (2010).
21. N. N. Achasov and A. A. Kozhevnikov, Pis'ma v ZhETF **91**, 611 (2010) [JETP Lett. **91**, 543 (2010)].
22. N. N. Achasov and A. A. Kozhevnikov, Phys. Rev. D **83**, 113005 (2011).
23. N. N. Achasov and A. A. Kozhevnikov, Nucl. Phys. B (Proc. Suppl.) **225–227**, 10 (2012).
24. N. N. Achasov and A. A. Kozhevnikov, Pis'ma v ZhETF **96**, 627 (2012) [JETP Lett. **96**, 559 (2012)].
25. N. N. Achasov, Yad. Fiz. **74**, 458 (2011) [Phys. Atom. Nucl. **74**, 437 (2011)].
26. N. N. Achasov, Teor. Mat. Fiz. **170**, 49 (2012) [Theor. Math. Phys. **170**, 39 (2012)].